CONCRETE STRUCTURAL HEALTH MONITORING IN NUCLEAR POWER PLANTS

Vivek Agarwal[1]
[1]Idaho National Laboratory
2525 Fremont Avenue, Idaho Falls, ID, 83401

Kyle D. Neal,[2] **Sankaran Mahadevan,**[2] **and Douglas Adams**[2]
[2]School of Civil and Environmental Engineering
Vanderbilt University, Nashville, TN, 37235

ABSTRACT

Assessment and management of aging concrete structures in nuclear power plants require a more systematic approach than simple reliance on existing code margins of safety. Health monitoring of concrete structures is performed in order to understand the current condition of a structure based on heterogeneous measurements and produce high-confidence actionable information regarding structural integrity. This information can be used to support operational and maintenance decisions. This paper describes a framework of research activities for health monitoring of nuclear power plant concrete structures. The proposed framework consists of four elements: (1) health monitoring, (2) data analytics, (3) uncertainty quantification, and (4) prognosis. The goal of this framework is to enable plant operators to make risk-informed decisions about structural integrity, remaining useful life, and performance of concrete structures across the nuclear fleet. Among several concrete degradations, research focuses on degradation caused by the alkali-silica reaction (ASR). ASR is a chemical reaction that, in the presence of sufficient moisture, forms a gel that increases in volume and exerts an expansive pressure inside the material, thus causing micro to macro-cracks. This paper also presents development of controlled concrete samples with reactive aggregates to cause ASR degradation and application of different non-destructive evaluation techniques to detect the damage caused by ASR. Initial results are presented in the paper along with a potential path forward.

Key Words: Alkali-silica reaction, concrete structural health monitoring, probabilistic framework, non-destructive techniques

1 INTRODUCTION

One challenge for the current fleet of light water reactors in the United States is age-related degradation of their passive assets, which includes concrete, cables, piping, and the reactor pressure vessel. As the current fleet of nuclear power plant continues to operate up to 60 years or beyond, it is important to understand the current and future health condition of passive assets under different operating conditions that would support operational and maintenance decisions. To ensure long-term safe and reliable operation of the current fleet, the U.S. Department of Energy's Office of Nuclear Energy funds the Light Water Reactor Sustainability Program to develop the scientific basis for extending operation of commercial light water reactors beyond the current license extension period.

Among the different passive assets of interest in nuclear power plants, concrete structures are investigated during this research project. Reinforced concrete structures found in nuclear power plants can

be grouped into four categories: (1) primary containment, (2) containment internal structures, (3) secondary containments/reactor buildings, and (4) spent fuel pool and cooling towers. These concrete structures are affected by a variety of degradation mechanisms that are related to chemical, physical, and mechanical causes and to irradiation. Age-related degradation of concrete results in gradual microstructural changes (e.g., slow hydration, crystallization of amorphous constituents, and reactions between cement paste and aggregates). Changes over long periods of time must be measured, monitored, and analyzed to best support long-term operation and maintenance decisions.

Structural health monitoring of concrete structures aims to understand the current health condition of a structure based on the heterogeneous measurements for producing high-confidence actionable information regarding structural integrity and reliability. To achieve this research objective, Vanderbilt University, in collaboration with Idaho National Laboratory and Oak Ridge National Laboratory, is developing a probabilistic framework for health monitoring of nuclear power plant concrete structures subject to physical, chemical, and mechanical degradation. This paper focuses on degradation caused in concrete by alkali-silica reaction (ASR). Specimens with ASR degradation are prepared to demonstrate the framework using several monitoring techniques at Vanderbilt University's Laboratory for Systems Integrity and Reliability. Through a demonstration example this paper showcases the effectiveness of the proposed concrete structural health monitoring framework.

2 PROBABILISTIC FRAMEWORK

The proposed systematic approach for assessing and managing aging concrete structures requires an integrated framework (shown in Fig. 1), including four elements: (1) monitoring, (2) data analytics, (3) uncertainty quantification, and (4) prognosis. The framework elements are briefly discussed in the following subsections. For details on each element of the proposed framework, refer to [1]. This framework will enable plant operators to make risk-informed decisions on structural integrity, remaining useful life, and performance of the concrete structure.

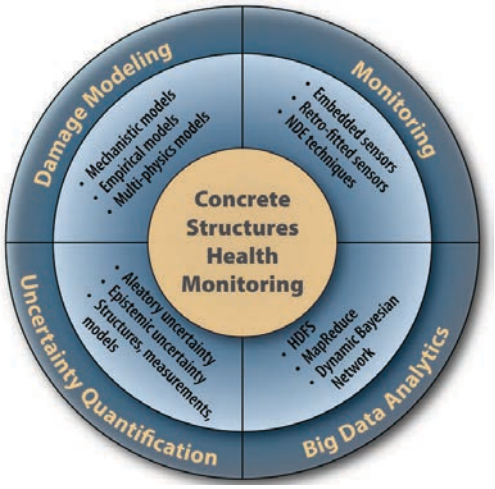

Figure 1. Elements of concrete structural health monitoring.

2.1 Monitoring

This element explores an effective combination of promising structural health monitoring techniques for full-field multi-physics monitoring of concrete structures. Optical, thermal, acoustic, and radiation-based techniques are being investigated for full-field imaging. Examples of these techniques include digital image correlation (DIC), infrared imaging, velocimetry, ultrasonic, and x-ray tomography. A

particular consideration is the linkage of chemical degradation mechanisms to observed degradation, which requires synergy between monitoring and prognosis.

2.2 Data Analytics

Information gathered from multiple health monitoring techniques results in a high volume, rate, and variety (i.e., heterogeneity) of data. This element leverages big data techniques to store, process, and analyze heterogeneous data (i.e., numerical, text, and image) and arrive at effective inference of concrete degradation. The data analytics framework can also integrate information from model prediction, laboratory experiments, plant experience and inspections, and expert opinion. Data mining, classification and clustering, feature extraction and selection, and fault signature analyses with heterogeneous data can be orchestrated through a Bayesian network for effective inference.

2.3 Uncertainty Quantification

This element quantifies uncertainty in health diagnosis and prognosis in a manner that facilitates risk-management decisions. Sources of natural variability, data uncertainty, and model uncertainty that arise in both modeling and monitoring activities can be considered and their effects quantified. In addition to measurement and processing errors, data uncertainty due to sparse and imprecise data for some quantities and due to large data on other quantities (i.e., data quality, relevance, and scrubbing) can be considered. Model uncertainty in multi-physics degradation modeling due to model form assumptions, unknown model parameters, and solution approximation errors can be included. Various uncertainty sources do not combine in a simple manner, and the Bayesian network offers a systematic approach for comprehensive uncertainty quantification in a manner that is informative to the decision-maker for operation, maintenance, inspection, and other risk-management activities.

2.4 Prognosis

This element leverages modeling of chemical, physical, and mechanical degradation mechanisms (such as alkali-aggregate reaction, chloride penetration, sulfate attack, carbonation, freeze-thaw cycles, shrinkage, and radiation damage) in order to assist monitoring and risk management decisions. Alkali-aggregate reaction currently is receiving prominent attention; however, other appropriate damage mechanisms for nuclear power plant concrete structures can be included. This element leverages modeling and computational advances and combined-physics experiments and integrates multiple models through an appropriate simulation framework. This combined model can be used for a prognosis of damage based on the present state of damage obtained from the diagnosis result. The uncertainty quantification in the diagnosis can be propagated through the prognosis model to quantify uncertainty in the prognosis.

3 DEVELOPMENT AND IMPACT OF ALKALI-SILICA REACTION

ASR is a reaction in concrete between the alkali hydroxides (K^+ and Na^+) in the pore solution and the reactive non-crystalline (amorphous) silica (S^{2+}) found in many common aggregates, given sufficient moisture. This reaction occurs over time and causes expansion of the altered aggregate through formation of a swelling gel of calcium silicate hydrate (C-S-H). Reactive silica is mainly provided by reactive aggregates and alkalis by the cement clinker. ASR swelling results from a relative volume increase between the product and reactant phases involved in the chemical reaction. First, the products expand in the pores and micro-cracks of the cementatious matrix. Once this free expansion space is filled, swelling is restrained and the product phases exert a local pressure on the surrounding concrete skeleton (Ulm 2000). Fig. 2 depicts the mechanism of ASR [2].

With water presence, the ASR gel increases in volume and exerts an expansive pressure inside the material, causing spalling micro to macro-cracks (due to non-homogeneous swelling related to

non-uniform moisture distribution). As a result, ASR reduces the stiffness and tensile strength of concrete, because these properties are particularly sensitive to micro-cracking. ASR also can cause serious cracking in concrete, resulting in critical structural problems that can even force demolition of a particular structure. The serviceability of concrete structures includes resistance to excessive deflections and a host of other durability concerns that can shorten the service life of a structure. Large surface crack widths and deep penetration of open surface cracks promote ingress moisture and any dissolved aggressive agents (such as chlorides). Additionally, the loss of concrete stiffness and potential for reinforcement yield are concerns for concrete deflection capabilities.

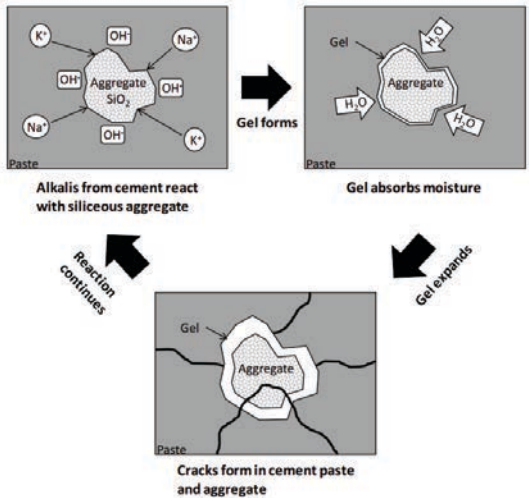

Figure 2. Mechanism of ASR [2].

Concrete core testing was conducted at the Seabrook nuclear power plant in February 2011 as part of the license renewal submission [3]. These tests confirmed the presence of ASR-induced cracks in various structures within the plant and reduced modulus to some extent. The impact of reduced modulus on ASR-affected structures was evaluated. This evaluation found that the overall structural integrity was still within the strength requirements.

4 EXPERIMENTAL CONCRETE SAMPLE

ASR is a slowly developing process that can take several decades to become visible and result in failure. In the laboratory, aggressive conditions are applied to accelerate this process so degradation progression and corresponding data can be observable. In this study, the NaOH in the mix water or placing the cured concrete in a NaOH solution is used to create a concrete pore solution with an increased pH that is capable of inducing ASR. At the same time, highly reactive siliceous aggregates, or glass, are used to provide an enriched source of silica. In addition, the relative humidity in concrete is essential for ASR, affecting both kinetics and magnitude. Water plays the role of solvent for silica dissolution and intervenes as the transport media for diffusion of ions through the pore solution. Water is also a necessary compound for formation of various reaction products (e.g., gels, precipitates, crystals, etc.). Finally, because ASR mechanisms are thermo-activated, concrete specimens are cured at higher temperatures (i.e., 60 to 80°C) to accelerate ASR. The high concentration of alkali hydroxides and silica at high temperature promotes the occurrence of ASRs. The high curing temperature (i.e., greater than 70°C) also promotes the formation of internal sulfate attack [4]. Therefore, using these three accelerating features, the ASR gel can be produced in a laboratory environment, leading to cracks in concrete within several months.

Three 9 × 5 × 2-in. concrete bricks (designated U1, U2, and U3) were cast and development of ASR was monitored over time using several non-destructive examination techniques. Powdered silica was used for aggregate in the three concrete bricks in the ratio of four parts cement to one part silica by weight. Brick U1 was not subjected to NaOH, which causes increased alkalinity and promotes ASR; therefore, U1 represents a baseline specimen. Bricks U2 and U3 were exposed to NaOH, but through different means. Brick U2 was submerged in a NaOH bath per American Society of Testing and Materials (ASTM) C1567-13 specifications [5] during accelerated curing. Brick U3 was cast using an NaOH solution in water mix to increase alkali content to 1.25% by mass of cement according to ASTM C1293-08b [6] and was cured suspended over a tub of water to create 100% relative humidity. One goal of this study was to see which method of applying NaOH was more effective in promoting development of ASR. A summary of the composition and curing conditions for Bricks U1, U2, and U3 is presented in Table I.

Table I. Summary of composition and curing conditions for Bricks U1, U2, and U3.

Brick	Aggregate	Sodium Hydroxide	Accelerated Curing
U1	Powdered silica	None	None (baseline)
U2	Powdered silica	In curing bath	60°C, submerged in NaOH solution
U3	Powdered silica	Mix water	60°C, 100% relative humidity

5 NON-DESTRUCTIVE EXAMINATION TECHNIQUES

5.1.1 Infrared Thermography

Infrared thermography maps the thermal load path in a material. In the case of concrete, cracking, spalling, and delamination [7] all create discontinuity in the thermal load path. Additionally, rebar and tensioning cables can be easily detected due to the difference in thermal conductivity coefficients between steel and concrete [8]. Thermography has even been shown to detect debonding between the reinforcing steel and concrete. Infrared thermography can be either an active or passive monitoring technique. When heat is locally added to the structure to create a temperature gradient, it is referred to as active. If solar heat is used to produce the temperature gradient, it is considered passive. Passive infrared thermography is preferred because it is less energy intensive. The current study is investigating performance of infrared thermography as a means of identifying ASR. Infrared thermography study of Bricks U1, U2, and U3 is reported here (see Table 1 for a summary of the composition and curing conditions for these bricks).

The hypothesis is that formation of ASR should change heat conductivity within the brick. Therefore, a temperature difference should exist between the dry-cured and NaOH-water-cured bricks at each time stamp. The temperature difference between the dry-cured data and NaOH-water-cured data at each time stamp is selected to be the baseline temperature difference. The corresponding temperature differences for Bricks U2 and U3 are expected to be different from the baseline brick, U1. Based on the baseline brick, upper bound and lower bound values (at each point in time) were selected for the temperature difference between dry-cured data and NaOH-water-cured data. If the temperature difference was outside the bounds, then a change in heat conductivity was indicated, implying formation of ASR. To set boundaries, maximum and minimum values for temperature difference were selected among all pixels between the dry-cured data and NaOH-water-cured data at each time stamp.

Temperature measurements from an infrared camera were verified by readings from multiple thermocouples. Five thermocouples were installed on concrete samples at different locations (as shown in Fig. 3 for Brick B2) and temperature data were collected along with data from infrared imaging measurements for verification purposes. Post processing of infrared images did not impact the verification process. Fig. 4 shows temporal temperature profiles that are measured by thermocouple (i.e., circle symbols) and infrared-camera (i.e., solid line) at five thermocouple

locations for comparison at Positions 1 through 3. A similar profile was obtained at Positions 4 and 5 (for details refer to [9]). A decent match between the thermocouple and infrared-camera temperature measurements at all five locations indicates the infrared camera can be used to non-destructively measure the temperature of a concrete structure when installation of thermocouples is not possible or desirable.

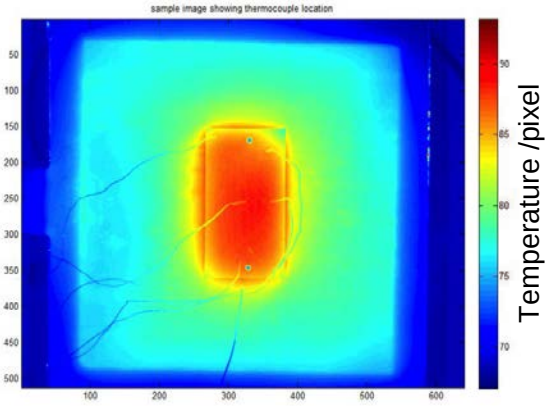

Figure 3. Thermal image of Brick U2 showing five thermocouple locations.

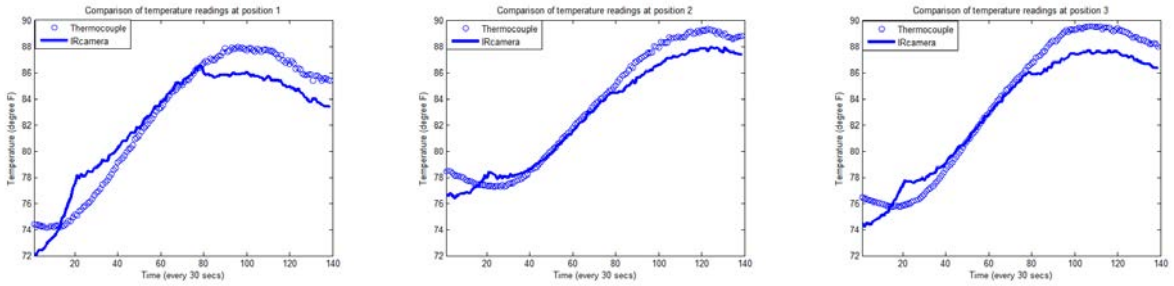

(a) (b) (c)

Figure 4. Comparison of infrared-camera and thermocouple measurements over a 30-second interval at (a) Position 1, (b) Position 2, and (c) Position 3.

5.1.2 Mechanical Deformation Measurement

The mechanical deformation measurement is a contact measurement technique. Calipers or an extensometer can be used to measure deformation along a linear distance. It is often convenient to glue on targets or cast nails into the concrete to provide more repeatable measurement points. In order to capture the ASR-induced concrete deformation, the measurement device needs to be accurate to within a few hundred microns. Most high-resolution mechanical measurement devices have a relatively short measuring span (i.e., 1 ft or less). This makes them ideal for laboratory experiments, but limits their applicability in real-world structures without using a significant number of targets glued to the structure.

The characteristic signature of ASR when damaging a concrete structure is expansion. Steel pegs were cast into the concrete bricks to provide points for repeatable measurements to be taken while the concrete was curing. Brick length measurements were taken multiple times as the bricks were curing. Fig. 5 tracks the length between the two steel pegs on each of the concrete bricks as a function of curing time. The baseline brick, U1, decreased in length, especially during the first month; length measurements

for the ASR-aggressive curing bricks (i.e., U2 and U3) show slight expansion. Reduction in length of the baseline U1 is associated with normal shrinkage of concrete over time, whereas the increase in length of accelerated ASR bricks, U2 and U3, indicates expansion of concrete due to formation of ASR gel.

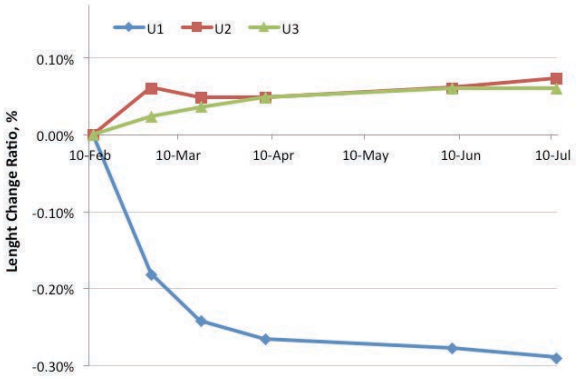

Figure 5. Change in length of bricks as a function of time.

5.1.3 Non-Linear Impact Resonance Acoustic Spectroscopy

Non-linear impact resonance acoustic spectroscopy (NIRAS) is a non-destructive testing technique that uses the vibrational response of a structure to classify damage. It was developed at Georgia Tech to detect ASR-induced damage in concrete [10]. NIRAS operates based on the following idea: a linear system has the same natural frequency regardless of the amplitude of the excitation force. This is not true for non-linear systems. In a non-linear system, the resonant frequency will shift depending on the amplitude of the excitation force. Because ASR causes micro-cracking within the concrete, which creates non-linearity, it is believed that NIRAS can be used to detect damage in concrete before cracking is visible on the surface. Because NIRAS is a global vibrational response technique (i.e., it measures shifts in resonant frequency), it is better suited for small laboratory concrete specimens than large concrete structures. For example, if a large concrete structure had a small patch of ASR growth, it is unlikely that NIRAS would be able to detect it is because it will have a minimal effect on the natural frequency of the structure.

Raw acceleration data are converted from the time domain to the frequency domain using the fast Fourier transform in MATLAB. In the frequency domain, the first resonant frequency was identified. The shift in resonance frequency of a concrete sample occurred when an increase in input force amplitudes indicated the concrete system was non-linear (i.e., there was micro-cracking due to ASR). The severity of concrete damage was characterized by non-linearity in the parameter, which was calculated by simply finding the scaled slope between the input force amplitude versus the frequency shift. It is well known that concrete samples with more severe damage generally have a larger non-linearity parameter (or steeper slope). If a sample is in pristine condition, it should have no frequency shift with increasing input force amplitude and the non-linearity parameter equals 0.

Brick U1 served as a baseline sample that was not exposed to NaOH. Brick U3 was exposed to water with an NaOH solution to increase the alkali content to 1.25% by mass of cement and was cured over a tub of water to provide 100% relative humidity. Fig. 6(a) shows the responses of Brick U3 in the frequency domain for various input force amplitudes ranging between 20 and 320 lb, which were taken on the first day of testing. The resonant frequency (at the peak of response) remained at the same level of 2,480 Hz as the impact force amplitude increased, which indicated the concrete structure was linear as expected. After 5 months of aggressive curing, Brick U3 exhibited a slight resonant frequency shift as the impact force amplitude increased (as shown in Fig. 6(b)) (the peaks moved to the left when input force

increased). Additionally, the resonant frequency at the lowest input force then increased to 2,800 Hz, which represents a large shift from resonance frequency at the beginning of the test (i.e., an increase of 320 Hz). This increase in resonant frequency might have been caused by the increase in stiffness of the concrete as it cured.

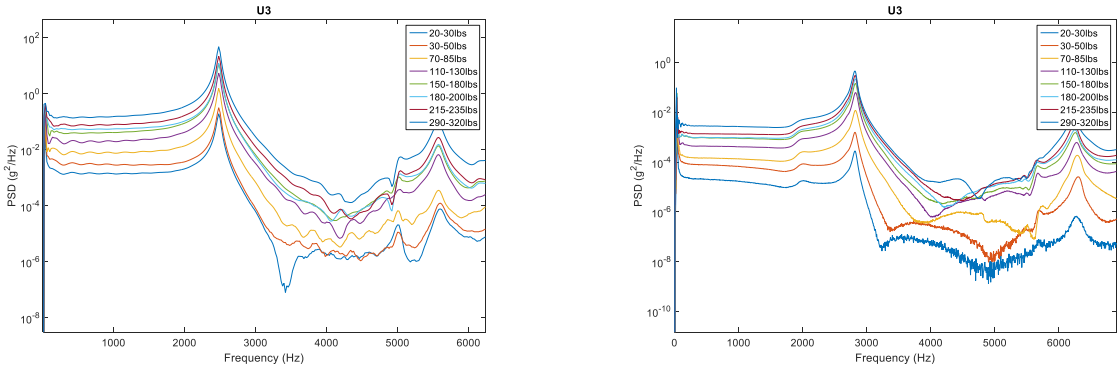

(a) (b)

Figure 6. Resonant frequency response observed for Brick U3 (a) on February 11 (Day 1 of the test) and (b) on February 11 (5 months later).

From the results, it is clear that damage was detected in Brick U3 after 5 months of ASR-accelerated curing. At that point, Brick U3 had expanded in length (green line in Fig. 5), which indicates the formation of ASR gel leading to concrete expansion instead of the concrete shrinkage that occurs during normal curing as in Brick U1 (blue line in Fig. 5). In this paper, the damage index was calculated as the ratio between the sideband amplitude and the pump amplitude (shown similarly to plots in Fig. 7). Figure 7 presents the non-linearity parameters of the three bricks calculated at different measurement dates. Initially, all three bricks (i.e., U1, U2, and U3) had a linear structure as indicated by the 0 non-linearity parameters. As the cure progressed, their non-linearity parameters increased over time, indicating the structures became non-linear. For details on the observations inferred from this analysis, refer to [9].

5.1.4 Vibro-Acoustic Modulation

Vibro-acoustic modulation (VAM) is vibrational-based non-destructive testing that has been successful in detecting non-linearities in various materials [11], but has not been used for concrete. We investigated the potential of using VAM in ASR detection of concrete bricks. VAM works by simultaneously exciting a structure with two frequencies of vibration. The low-frequency input is termed the “pump” and the high-frequency input is termed the “probe” [12]. Interaction of the pumping and probing signals indicates the presence of non-linearities in the system. Because the pumping signal causes the crack to open and close, the effective cross-sectional area the probing signal can travel through changes. Therefore, the amplitude of the probing signal is transmitted through the beam changes with the phase of the pumping signal. This modulation will produce side bands around the probing frequency.

During the VAM test, the modal hammer struck the bricks to create an impulsive load that was used as the low-frequency pump and the piezo-stack actuator acted as the high-frequency probe. The tri-axial accelerometer measured the sample’s response. A sampling frequency of 51.2 kHz facilitated the high-frequency probe and a sampling period of 0.1 seconds resolved the modulated sidebands. A probing frequency of 14 kHz was used, and the response from eight hammer impacts was averaged together.

Fig. 8(a) depicts the power spectral density (PSD) of Brick U3 taken after 5 months of accelerated curing. From the VAM results, as shown in Fig. 8(a), a damage index was calculated as the ratio of the sideband amplitude to the pump amplitude. The VAM damage indices of the three tested bricks at each

measurement date are given in Fig. 8(b). The data show increasing damage indices for each of the bricks over time.

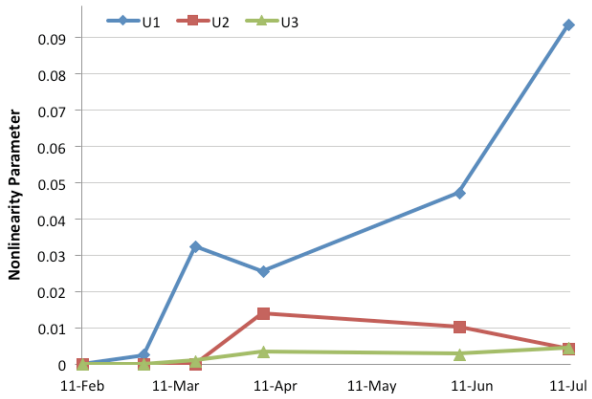

Figure 7. Nonlinearity parameters of Bricks U1, U2, and U3 as function of time.

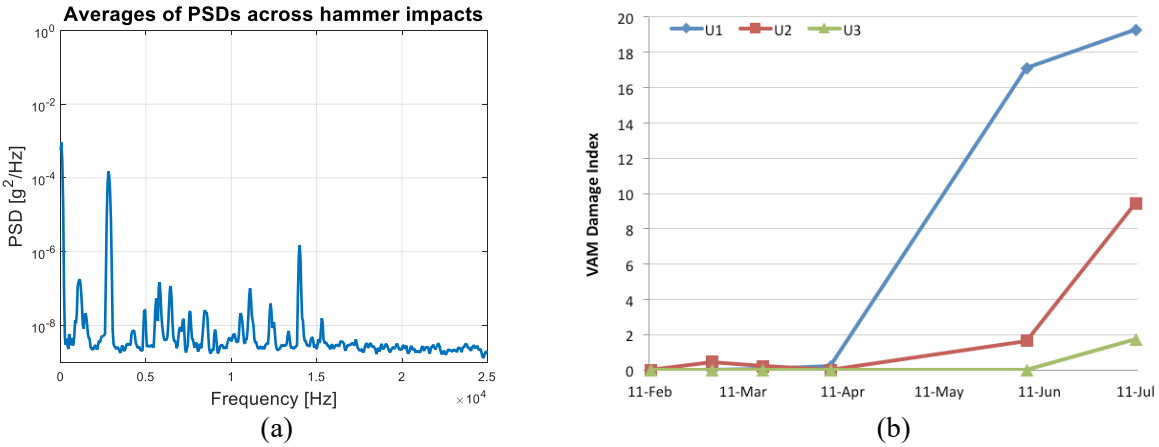

Figure 8(a). Average PSDs across different hammer impacts for Brick U3 after 5 months of curing and 8(b) VAM damage indices for Bricks U1, U2, and U3 as function of time.

6 CONCLUSIONS AND PATH FORWARD

This paper presented a series of experiments that were conducted at Vanderbilt University to provide sufficient degradation data in support of the framework for diagnosis of structure condition. The main activities involved developing a concrete sample with reactive aggregates and curing them under different conditions to accelerate the formation of ASR gel. Application of different non-destructive examination techniques, including mechanical deformation measurements, NIRAS, VAM, and infrared thermography, was studied for damage detection. Consistent experimental data from all non-destructive examination techniques indicate these techniques can be used to generate data related to an assessment of the degradation of concrete structures damaged by ASR.

As part of this ongoing research, some future work will focus on the following tasks: (1) localizing and quantifying damage and exploring embedded sensors (e.g., strain and pH), (2) collaborating with the University of Alabama on development of concrete specimens with distributed ASR aggregates and with localized ASR aggregates, (3) enhancing monitoring techniques to collect high-quality data to quantify

the onset of ASR and trend its progress within a concrete sample over a period of time, and (4) coordinating with ongoing research activities at the University of Tennessee, Knoxville, and Oak Ridge National Laboratory to construct and monitor a large mockup and, in particular, application of digital image correlation.

7 ACKNOWLEDGMENTS

This report was made possible through funding by the U.S. Department of Energy's Light Water Reactor Sustainability Program. We are grateful to Richard Reister of the U.S. Department of Energy and Bruce Hallbert and Kathryn McCarthy at Idaho National Laboratory for championing this effort.

8 REFERENCES

1. Mahadevan, S., V. Agarwal, K. Neal, D. Kosson, and D. Adams, 2014, *Interim Report on Concrete Degradation Mechanisms and Online Monitoring Techniques*, INL/EXT-14-33134, Idaho National Laboratory, September 2014.
2. Kreitman, K., 2011, "Nondestructive Evaluation of Reinforced Concrete Structures Affected by Alkali-Silica Reaction and Delayed Ettringite Formation," M.S. Thesis: University of Texas at Austin, Austin, Texas.
3. NextEra Energy Seabrook, 2012, "Impact of Alkali-Silica Reaction on Concrete Structures and Attachments," the Response to Confirmatory Action Letter, SBK-L-12106, from NextEra Energy Seabrook to the Nuclear Regulatory Commission, May 24, 2012.
4. Giannini, E. R. et al., 2012, *Non-Destructive Evaluation of In-Service Concrete Structures Affected by Alkali-Silica Reaction (ASR) or Delayed Ettringite Formation (DEF)—Final Report, Part I,* FHWA/TX-13/0-6491-1, Texas A&M Transportation Institute, http://library.ctr.utexas.edu/ctr-publications/0-6491-1.pdf, October 2013.
5. ASTM C1567-13, 2013, "Standard Test Method for Determining the Potential Alkali-Silica Reactivity of Combinations of Cementitious Materials and Aggregate (Accelerated Mortar-Bar Method)," ASTM International, 2013.
6. ASTM C1293-08b, 2015, "Standard Test Method for Determination of Length Change of Concrete due to Alkali-Silica Reaction," ASTM International, August 2015.
7. Renshaw, J., N. Muthu, and M. Guimaraes, 2014, "Thermographic Inspection of Concrete, Tanks, and Containment Liners," *EPRI Conference,* Charlotte, North Carolina, May 8, 2014.
8. Kobayashi, K. and N. Banthia, 2011, "Corrosion detection in reinforced concrete using induction heating and infrared thermography," *Journal of Civil Structural Health Monitoring*, **Vol**. 1, No. 2, pp. 25–35.
9. Agarwal, V., K. Neal, S. Mahadevan, B. T. Pham, and D. Adams, 2016, *Data Analysis of Different Nondestructive Testing Techniques to Monitor Concrete Structure Degradation due to Alkali-Silica Reaction*, INL/EXT-16-39915, Idaho National Laboratory, September 2016.
10. Lesnicki, K. J., J. Y. Kim, K. E. Kurtis, and L. J. Jacobs, 2014, "Characterization of ASR Damage in Concrete Using Nonlinear Impact Resonance Acoustic Spectroscopy Technique," *NDT&E International*, **Vol**. 44, No. 8, pp. 721–727.
11. Kim, S., D. E. Adams, H., Sohn, G. Rodriguez-Rivera, N. Myrent, R. Bond, J. Vitek, S. Carr, A. Grama, and J. J. Meyer, 2014, "Crack detection technique for operating wind turbine blades using Vibro-Acoustic Modulation," *Structural Health Monitoring*, **Vol**. 13, No. 6, pp. 660–670.